

Preparation and Characterization of Pectin Based Proton Exchange Membranes Derived by Solution Casting Method for Direct Methanol Fuel Cells

Mohanapriya Subramanian, V. Raj

Abstract—Direct methanol fuel cells (DMFCs) are considered to be one of the most promising candidates for portable and stationary applications in the view of their advantages such as high energy density, easy manipulation, high efficiency and they operate with liquid fuel which could be used without requiring any fuel-processing units. Electrolyte membrane of DMFC plays a key role as a proton conductor as well as a separator between electrodes. Increasing concern over environmental protection, biopolymers gain tremendous interest owing to their eco-friendly bio-degradable nature. Pectin is a natural anionic polysaccharide which plays an essential part in regulating mechanical behavior of plant cell wall and it is extracted from outer cells of most of the plants. The aim of this study is to develop and demonstrate pectin based polymer composite membranes as methanol impermeable polymer electrolyte membranes for DMFCs. Pectin based nanocomposites membranes are prepared by solution-casting technique wherein pectin is blended with chitosan followed by the addition of optimal amount of sulphonic acid modified Titanium dioxide nanoparticle (S-TiO₂). Nanocomposite membranes are characterized by Fourier Transform-Infra Red spectroscopy, Scanning electron microscopy, and Energy dispersive spectroscopy analyses. Proton conductivity and methanol permeability are determined in order to evaluate their suitability for DMFC application. Pectin-chitosan blends endow with a flexible polymeric network which is appropriate to disperse rigid S-TiO₂ nanoparticles. Resulting nanocomposite membranes possess adequate thermo-mechanical stabilities as well as high charge-density per unit volume. Pectin-chitosan natural polymeric nanocomposite comprising optimal S-TiO₂ exhibits good electrochemical selectivity and therefore desirable for DMFC application.

Keywords—Biopolymers, fuel cells, nanocomposite, methanol crossover.

I. INTRODUCTION

OWING to growing demand for clean and sustainable energy, fuel cells have been hyped as an eco-friendly, efficient alternate for conventional fossil fuel power sources. Specially, DMFCs that use renewable methanol as a fuel are recognized as an attractive source of power generation, owing to their high energy density, long lifetime, low pollution, portability and simplified system design [1], [2]. Permeation of methanol from anode to cathode through a proton exchange membrane (PEM) adversely affects DMFC efficiency. Nafion, state of art DMFC electrolyte incurs about 40% loss of fuel and a drop in open-circuit potential by as much as 0.15-0.2 V due to methanol cross-over [3]. Higher cost and non-

ecofriendly nature of Nafion limits its wide spread application. Therefore, continuous research efforts are stimulated in the direction of developing alternate low-cost PEMs. There exists a demand for environmentally-benign raw materials in the view of depletion of raw materials and fossil fuels, particularly the areas in which an increasing industrial requirement is expected. This emphasizes the significance of developing cost-effective, eco-friendly materials derived from natural sources such as polysaccharides, proteins, lipids, etc. Therefore, cost effective and eco-friendly polymer electrolytes from renewable sources can become a promising substitute for synthetic polymers for fuel cell applications. In the light of the foregoing, polysaccharides such as chitosan (CS), alginate, carrageenan and pectin (PC) are of meticulous interest, owing to their good film-forming capability along with inherent methanol-blocking characteristics. Many of the CS based PEMs have been successfully demonstrated for DMFC application as substantiated by our earlier studies [4]-[6]. PC is a least explored class of polysaccharides with respect to DMFC application, none other than a preliminary evaluation on the utility of amidated PC as a DMFC electrolyte is available in the literature [7]. Taking the advantage of eco-friendly and easy availability of PC, it is blended with CS polymer in order to fabricate polymeric membranes with adequate mechanical stability, ionic conductivity and methanol selectivity. Blending polymers are one of the most promising approaches owing to the fact that resulting blend restrains attractive features of individual component. At the same time, it diminishes their defective qualities. It is quite interesting to combine two different natural polymers. In order to further promote ionic conductivity, sulphonated titanium dioxide nanoparticles are (S-TiO₂) incorporated into the blends to formulate bionanocomposite membranes. It is illustrious that S-TiO₂ leads to an increase in net acid content by incrementing number ion-conducting groups per unit volume. The observed increase in IEC is due to the presence of hydroxyl (-OH) including isolated and bridged hydroxyl and sulphonic acid groups present over the TiO₂ surface [8].

Purpose of this investigation is to develop PC-CS biopolymer based nanocomposite membranes, evaluating their functional properties such as proton conductivity and methanol permeability as well as substantiating their suitability as a DMFC electrolyte. These membranes are rationally designed to possess higher selectivity for conducting protons rather than methanol.

Mohanapriya Subramanian is with the Periyar University, India (e-mail: priyaachem@gmail.com).

II. EXPERIMENTAL

A. Materials

PC (M. Wt 3.0×10^4 – 1.0×10^5) was obtained from Loba Chemie, India. Hydrophilic fumed TiO_2 , with an average particle size of 21 nm was procured from Aeroxide chemicals, India. Sulfosuccinic acid (SSA) and methanol were obtained from SRL chemicals, India. Glutaraldehyde (25% aqueous) and sulfuric acid (98%) were obtained from S.D. Fine Chemicals, India. All the chemicals were used as received. De-ionized (DI) water (Resistivity $18.4 \text{ M}\Omega \text{ cm}$) from Millipore was used during the experiments.

B. Membrane Preparation

1) Preparation of S- TiO_2

Surface modification of TiO_2 was carried out, and 1 g of TiO_2 nanoparticles was added to 15 mL of 0.5 M sulfuric acid. Then, it was kept under ultrasonication for 1h. Solid mass was filtered and washed thoroughly with de-ionized water until filtrate becomes neutral to remove residual acid. S- TiO_2 was obtained by drying the sample at 80°C for 24h.

2) Preparation of PCCS Nanocomposite

PCCS nanocomposite membranes were prepared by solution-casting technique. Briefly, 1 wt.% CS solution was prepared by dissolving 1 g of CS in water followed by stirring until a clear solution was obtained. Similarly, 20 ml of 25 wt.% PC relative to CS was dissolved in de-ionised water followed by stirring until a homogeneous solution was obtained. Both the solutions were mixed together and stirred for 3-4h to form a compatible blend. Required quantity of S- TiO_2 was dispersed in de-ionised water under ultra sonication for 2h. The resultant solution was added drop-wise to the above PC-CS blend solution under continuous stirring for 24h. Sequential binary cross-linking with a mixture which consists of 10 wt.% sulfosuccinic acid (SSA), and 5 wt.% glutaraldehyde (GA) was done. The resulting solution was cast as a membrane on a flat Plexiglass plate by evaporating solvent at room temperature. PC-CS blend membranes were prepared in the similar manner without addition of S- TiO_2 . The composition of S- TiO_2 was varied from 1 wt.% to 5 wt.% in PC-CS nanocomposite membranes comprising 1 wt.%, 3 wt.%, and 5 wt.% of S- TiO_2 which are designated as PCCS-I, PCCS-II and PCCS-III respectively.

C. Ion-Exchange Capacity, Sorption and Proton Conductivity Measurements

Ion-exchange capacity (IEC) specifies the number of milliequivalent of ions in 1 g of the membrane. IEC for the membranes was determined by following the procedure reported in the literature, and the IEC is calculated using

$$\text{IEC} = \frac{(B - P)0.01 \times 5}{m} \quad (1)$$

where B is the amount of sulfuric acid used to neutralize blank sample solution in mL, P is amount of H_2SO_4 used to neutralize the membranes soaked solution in mL, N is

normality of H_2SO_4 , 5 is the factor corresponding to the ratio of the amount of NaOH used to soak nanocomposite membranes to the amount used for titration, and m is membrane mass in g.

D. Sorption and Proton Conductivity Measurements

Sorption measurements were conducted by immersing circularly-cut membrane samples into de-ionized water for 24h to attain equilibrium and weighed (diameter = 2.5 cm) before dipping into sorption chamber. The membranes were surface blotted, and their sorbed weights were measured. Sorption values for aforesaid membranes were calculated using (2):

$$\text{Sorption} = \left(\frac{W_\infty - W_0}{W_0} \right) \quad (2)$$

In (2), W_∞ and W_0 refer to the weights of sorbed and dry membranes, respectively. The experiments were repeated for at least three different membrane samples, and average value was considered.

Proton conductivity measurements were carried out with PC-CS blend, PCCS nanocomposite membranes in a four-probe conductivity cell by AC impedance technique. The conductivity cell comprised two electrodes, each of 20 mm diameters. The membrane was placed between these two electrodes to have a through plane contact and then mounted in a Teflon block and kept in a closed glass-container filled with water to maintain 100% humidity which also has the provision to heat. The membranes were equilibrated for 24h in this condition before measuring ionic conductivity. Conductivity measurements were done by varying the temperature from 30°C to 100°C . AC impedance spectra for the membranes were recorded in the frequency range between 1 MHz and 10 Hz with an amplitude of 10 mV using an Autolab PGSTAT 30. The resistance (R) of the membrane was determined from the high-frequency intercept of the impedance with the real axis and the membrane conductivity was calculated from the membrane resistance, R, using (3) as:

$$\sigma = \left(\frac{1}{R \times A} \right) \quad (3)$$

In (3), σ is the proton conductivity of the membrane in S/cm, l is the membrane thickness in cm, and A is the membrane cross sectional area in cm^2 .

E. Physicochemical Characterization

Mechanical properties of the membranes were studied using Universal testing machine (UTM) (Model AGS-J, Shimadzu) with an operating head-load of 10 kN. ASTM D-882 standards were followed to cut the test samples in dumb-bell shape. Membranes were then placed in the sample gauze of the machine. The film was stretched at a cross-head speed of 1 mm/min, and its tensile strength was estimated using

$$\text{Tensile Strength} = \frac{\text{Maximum Load}}{\text{Cross-sectional area}} \quad (4)$$

Surface morphologies of PCCS blend and PCCS nanocomposite membranes were studied using JEOL JSM 35CF Scanning Electron Microscope (SEM). Gold film of thickness < 100 nm was sputtered on the membrane surfaces using a JEOL Fine Coat Ion Sputter-JFC-1100 Unit, before subjecting it to actual measurements.

FTIR spectra for TiO₂ powder, S-TiO₂, and PCCS-II nanocomposite membranes were recorded using a Nicolet IR 860 spectrometer (Thermo Nicolet Nexus-670) in the frequency range between 4000 and 400 cm⁻¹.

F. Methanol Permeability

A diffusion cell consists of two 50 mL chambers in which one compartment was filled with 2 M methanol solution and the other with deionised water. The membrane (effective area 4 cm²) was clamped between the two compartments which were kept under stirring for 12h during experiment. The apparent methanol permeability of the membranes was measured at 70 °C by conducting density measurements of liquids. The variation of methanol concentration with time in the receiver reservoir (C_B) was determined by means of density measurements. Amount of permeated methanol from donor reservoir (C_A) to receiver reservoir (C_B) was calculated by determining the difference in the density of methanol before and after conducting the experiment. The densities of methanol were measured using a density meter (Mettler Toledo, DB51) by taking 20 mL of the collected methanol sample. The molarity of the methanol was calculated from the measured density values using (5):

$$\text{Molarity} = 10 \times \text{wt.\% of Methanol} \left(\frac{\rho}{M} \right) \quad (5)$$

where 'ρ' is the density of methanol (g/cm³), and 'M' is the molecular weight of methanol (g/mol). Accordingly, methanol permeability (P) was calculated as:

$$P = \left(\frac{V_B \times l}{A \times C_{AO}} \right) \times S \quad (6)$$

where V_B is the volume of the receptor compartment, and l, A, and C_{AO} are the membrane thickness, effective membrane area and feed concentration, respectively.

III. RESULTS AND DISCUSSIONS

A. Characterization of TiO₂ Nanoparticles

Fig. 1 compares FTIR spectra of pure TiO₂ with that of S-TiO₂. Spectrum of S-TiO₂ is associated with prominent characteristic -SO₃H absorption located at 1000-1100 cm⁻¹, and it coincides with absorption band of symmetric and asymmetric O=S=O of -SO₃H group. Also, characteristic peaks due to -OH stretching are widened owing to the formation of hydrogen bonds.

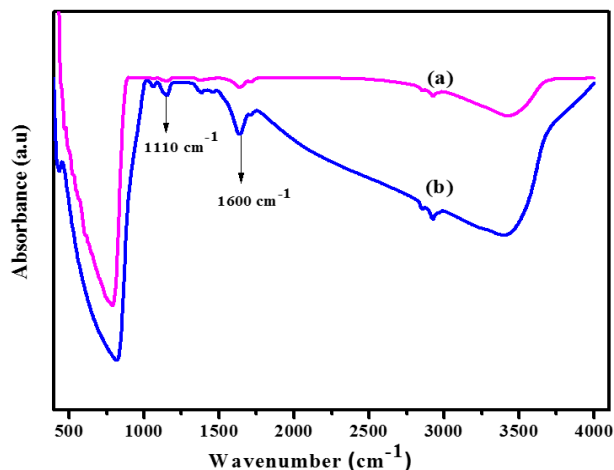


Fig. 1 FTIR spectra for (a) pure TiO₂ nanoparticles and (b) S-TiO₂ nanoparticles

Fig. 2 consists of SEM image of S-TiO₂ and corresponding EDAX data of S-TiO₂ nanoparticle. Clear spherical nanostructure with a grain size of approximately 30 nm is visible from the SEM image. EDAX data with sulphur peaks prove that TiO₂ nanoparticles are surface modified with -SO₃H groups.

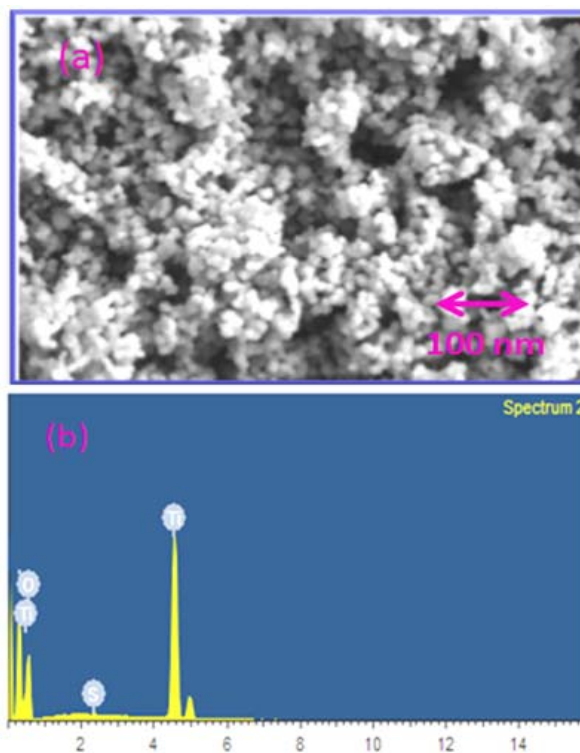


Fig. 2 (a) SEM morphology of S-TiO₂ nanoparticles and (b) corresponding EDAX data

B. Characterization of Polymer Membranes

Fig. 3 represents FTIR spectra of PC, PC-CS blend, and PCCS-II nanocomposite membranes. Spectrum of pure PC

exhibits a broad band at $3800\text{--}2300\text{ cm}^{-1}$ related to stretching vibrations of O-H and C-H groups. Change in characteristic outline of CS spectrum as well as shifting of peak to lower frequency range due to hydrogen bonding between –OH and –NH₂ groups of CS and –OH groups of PC is evident from FTIR.

FTIR spectra of PC-CS polymeric blend possess two relatively broad bands appear in the region $1800\text{--}1600\text{ cm}^{-1}$, which can be ascribed to the overlapping of bands due to amino and carboxylic groups of CS with hydroxyl groups of PC. An intense peak at 1620 cm^{-1} is ascribed to interchain or intermolecular ionic salt bonds appear due to formation of polyelectrolyte complex, which is produced by electrostatic interaction between positively charged amino groups on C2 of CS (pyranose ring) and negatively charged carboxyl groups of C5 of PC pyranose ring. A spectrum of PCCS-II represents combined spectral features of both PC-CS blend and S-TiO₂ nanoparticles. No obvious changes in the characteristic vibrations are observed due to incorporation of S-TiO₂ pointing to that basic framework chemical structure remains unchanged after modification information about intermolecular interactions between polymers and successful interaction of polymer blends with S-TiO₂ nanoparticles.

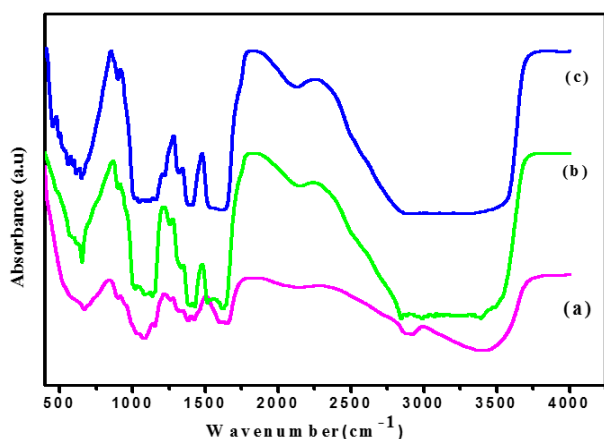


Fig. 3 FTIR spectra for (a) CS (b) PCCS and (c) PCCS-II nanocomposite membranes

C. Sorption and IEC Studies on Membranes

Sorption data associated with PCCS blend and PCCS nanocomposites measured at $70\text{ }^{\circ}\text{C}$ with water are shown in Fig. 4. Carboxyl group of PC molecule ionically interacts with functional groups of CS creating large inter-connected structure which provides more space for water binding to the material itself, thereby increasing water uptake.

Carboxylic group itself is a hydrophilic functional group therefore contributes to water-binding capability of membrane. Also, it is noteworthy that degree of water uptake has been considerably increased after incorporating S-TiO₂ nanoparticles, which demonstrates tendency of TiO₂ to absorb water molecules.

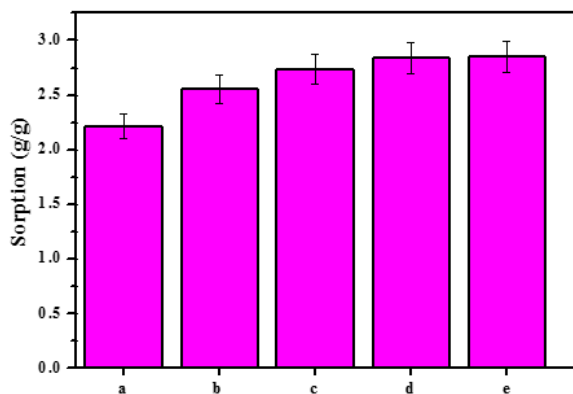


Fig. 4 Sorption properties of (a) CS (b) PC-CS (c) PCCS-I (d) PCCS-II (e) PCCS-III

IEC is an important property of membranes which is determined by appropriate segregation of hydrophilic and hydrophobic nanodomains to form per location paths for proton transport. Concentration of ion-exchangeable groups has been increased upon addition of S-TiO₂ into polymeric blends. The results suggest that quantity and density of S-TiO₂ nanoparticles on the membrane surface directly influence the efficiency of surface modification and ionic conductivity through reducing water permeation resistance.

Tensile strength and elongation for PCCS nanocomposite membranes are shown in Table I. It is evident from the data that blending PC causes only marginal improvement in tensile strength of PC-CS polymeric blend, but its elongation properties are enhanced considerably. Blending PC constitutes additional hydrogen bonds in the membrane framework, which perform as reinforcing bridge elements.

TABLE I
PROPERTIES OF MEMBRANES

Membrane type	IEC (meq.g)	Tensile strength (MPa)	Elongation - at-Break (%)	Arrhenius Activation energy (kJ/mol)
PCCS	0.48	20	34	29.7
PCCS-I	0.59	31	27	26.7
PCCS-II	0.73	32	28	21.9
PCCS-III	0.68	33	27	22.3

PC-CS polymer blend displayed better elongating properties than their respective constituents. Nevertheless, when S-TiO₂ nanoparticle is incorporated, elongation properties of nanocomposite membranes tend to decrease because it hinders the free movement of polymer chains. PCCS-II nanocomposite membrane displays maximum tensile strength along with good elongation characteristics, which is essentially ascribed to the strong interaction between organic and inorganic phases.

D. Proton Conductivity Measurements

Fig. 5 shows the proton conductivities of all membranes measured at different temperatures from $30\text{ }^{\circ}\text{C}$ to $100\text{ }^{\circ}\text{C}$. Apparently, proton conductivity of PC has been enhanced by

blending with CS polymer and incorporation of S-TiO₂ into polymer blend further promotes proton conductivity.

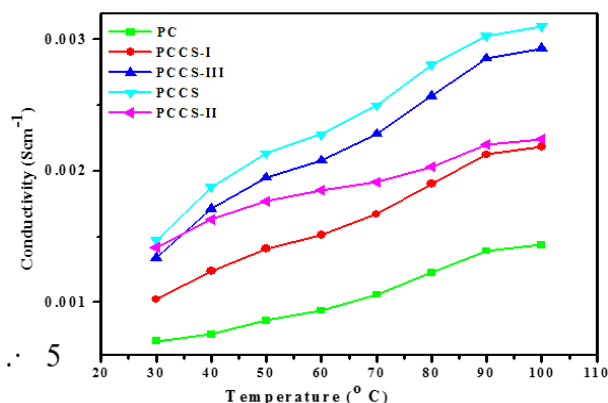


Fig. 5 Variation of proton conductivity with temperature

Combining PC with CS generates a flexible polymer framework, and the resulting blend offers more space for water molecules to reside. These water molecules facilitate ionic mobility. In the other words, appropriate balance between hydrophobic and hydrophilic domains is established in PC-CS polymer matrix, which allows a fast exchange between mobile ions and fixed charged sites through hydrated hydrophilic network. S-TiO₂ nanoparticle promotes proton conduction both through hopping and vehicular mechanism. They rapidly transmit protons through inter-linking hydrophilic domains. It is noteworthy that -SO₃H functional groups present in SSA (cross-linking agent) also involved in hydrogen bonding, thereby increasing the density of hydrogen bonding network. Vehicular transfer of protons is also facilitated as bridged water complexes are formed in the nanocomposites. Hence, proton conductivity of membranes followed the sequence: PC < PC-CS < PCCS-I < PCCS-II ≈ PCCS-III. When S-TiO₂ is added in excess, proton conductivity decreases due to aggregation of additive in the polymer matrix.

All the membranes show an Arrhenius-type temperature dependence of proton conductivity indicating thermally-activated process. The activation energy (E_a), which is the minimum energy, required for proton transport, is obtained from the slope of Arrhenius plots by plotting $\ln \sigma$ vs. $1/T$ according to (7):

$$\sigma = \sigma_0 e^{-(E_a / RT)} \quad (7)$$

In (6), σ is the proton conductivity, σ_0 is the pre-exponential factor, E_a is the activation energy in (kJ/mol), R is the universal gas constant (8.314 J/mol K), and T is the absolute temperature (K). As represented in Fig. 6, conductivity increases with increasing temperature pointing out that the proton conductivity is a thermally activated process. E_a values for all the membranes are given in Table I. From the data, it is obvious that E_a associated with proton conduction decreases

after incorporation of S-TiO₂ nanoparticles into polymeric blend.

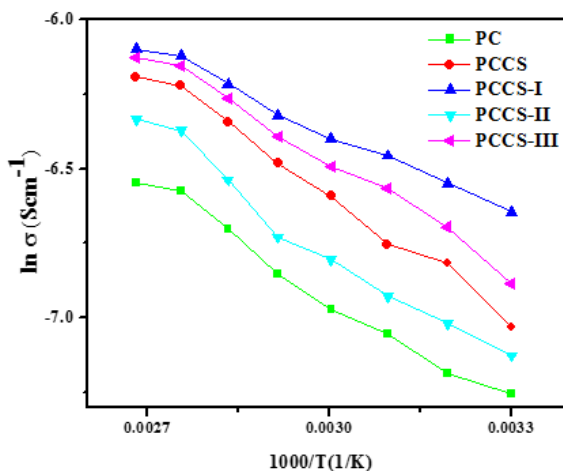


Fig. 6 Arrhenius plot of $\ln \sigma$ vs. $1000/T$

E. Methanol Permeability and Electrochemical Selectivity

Fig. 7 shows methanol permeability data for PC-CS based membranes. Methanol permeability values through PCCS nanocomposite membranes have rapidly decreased by nearly 40% due to presence of S-TiO₂. Due to the transformation in the microstates, methanol conducting path has been turned into a tortuous one instead of direct pathway. As a result, methanol permeability through the membrane decreased.

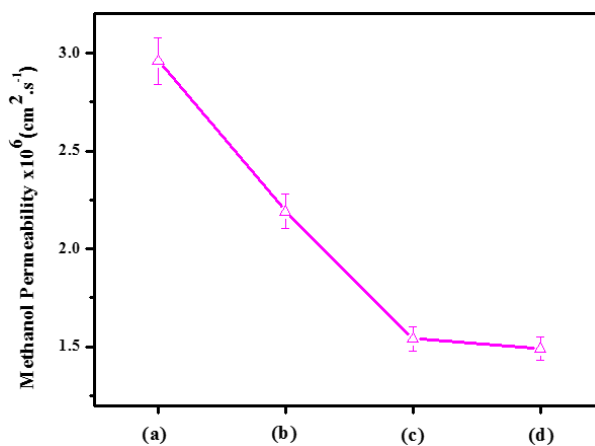


Fig. 7 Methanol permeability of (a) PC-CS (b) PCCS-I (c) PCCS-II (d) PCCS-III

It is important to note that methyl ester groups belong to PC could exert a hydrophobic repulsion towards methanol molecules therefore helpful for preferential sorption of water from aqueous methanol. In addition, dispersed S-TiO₂ nanoparticles create closely packed network with lower volume of free-void space, which effectively block passage of methanol molecules [9].

Electrochemical selectivity of membranes for protons over methanol can be defined as the proton conductivity (σ) divided

by methanol permeability (P), which is often used to evaluate the membrane-electrolyte performance in DMFC.

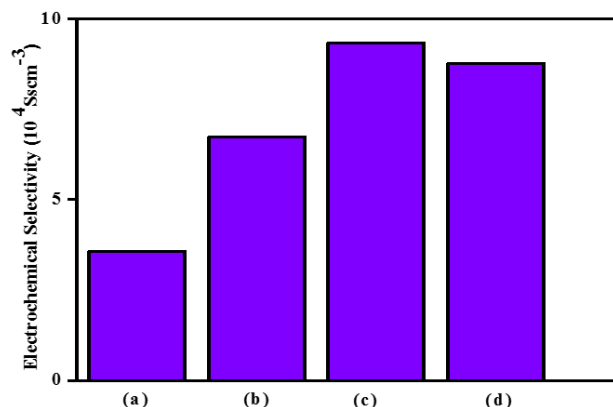


Fig. 8 Methanol permeability of (a) PC-CS (b) PCCS-I (c) PCCS-II (d) PCCS-III

From Fig. 8, it is apparent that, due to the increase in proton conductivity and decrement in methanol cross-over flux, selectivity values of PCCS-II nanocomposite membrane are higher compared to other membranes under study.

IV. CONCLUSIONS

PC based cost-effective natural polymeric blends tailored with S-TiO₂ nanoparticles to realize a composite membrane for application in DMFCs have been explored. PC transforms morphological properties of CS, results in construction of a slackly-packed network with higher affinity for water, which greatly reduces methanol permeation. Fine dispersion of S-TiO₂ increases the compactness of ion-conducting groups resulting in nanocomposites ultimately appropriate for DMFC application. Low-cost eco-friendly components, ready availability and convenient method of preparation are essential highlights of these kinds of membranes.

REFERENCES

- [1] V. Neburchilov, J. Martin, H. Wang, J. Zhang, "A review of polymer electrolyte membranes for direct methanol fuel cells," *J. Power Sources*, vol.169, no., pp. 221–238, Apr. 2007.
- [2] V. Radenahmad, A. Afif, P. I. Petra, S.M.H. Rahman, S. G. Eriksson, A. K. Azad, "Proton-conducting electrolytes for direct methanol and direct urea fuel cells-A state-of-the-art review," *Renew. Sustainable Energy Rev.*, vol.57, no., pp.1347–1358, May. 2016.
- [3] S. P. Jiang, Z. G. Liu, Z. Q. Tian, "Layer-by-Layer Self-Assembly of Composite Polyelectrolyte–Nafion Membranes for Direct Methanol Fuel Cells" *Adv. Mater.*, vol.18, no.8, pp.1068–1072, Apr 2006.
- [4] A. Muthumeenal, S. Neelakandan, P. Kanagaraj, A. Nagendran, "Synthesis and properties of novel proton exchange membranes based on sulfonated polyethersulfone and N-phthaloyl chitosan blends for DMFC applications" *Renew. Energy*, vol.86, pp.922–929, Sep 2016.
- [5] S. Mohanapariya, S. D. Bhat, A. K. Sahu, S. Pitchumani, P. Sridhar and A. K. Shukla, "A New mixed matrix membrane for DMFCs" *Energy and Environ.Sci.*, vol. 2, no.11, pp.1210–1216, Sep 2009.
- [6] S. Mohanapariya, A. K. Sahu, S. D. Bhat, S. Pitchumani, P. Sridhar, C. George, N. Chandrakumar and A. K. Shukla, "Bio-composite membrane Electrolytes for Direct Methanol Fuel Cells", *J. Electrochem. Soc.*, vol.158, no.11, pp. B1319–B1328, Sep 2011.
- [7] R. K. Mishra, A. Anis, S. Mondal, M. Dutt, A. K. Banthia, "Preparation and Characterization of Amidated Pectin based Polymer Electrolyte Membranes", *Chinese J. Polym.Sci.*, vol.27, no.5, pp.639–646, Oct 2009.
- [8] C. Deina, E. Fois, S. Coluccia, G. Martra, "Surface structure of TiO₂ P25 Nanoparticles: Infrared study of Hydroxy Groups on Coordinative Defect Sites *J. Phy. Chem C.*, vol.114, no.49, pp.21531–21538, Nov 2010.
- [9] M. Sairam, M.B. Patil, R. S. Veerapur, S. A. Patil, T. M. Aminabhavi, "Novel dense poly(vinyl alcohol)–TiO₂ mixed matrix membranes for pervaporation separation of water–isopropanol mixtures at 30°C", *J. Membr. Sci.*, vol.281, no.1, pp.95–102, Sep 2006.